CENTRAL ASIAN JOURNAL OF MATHEMATICAL THEORY AND COMPUTER SCIENCES

https://cajmtcs.centralasianstudies.org

Volume: 03 Issue: 07 | July 2022 **ISSN: 2660-5309**

RADIATION-BRINKMAN NUMBER EFFECTS ON BLOOD FLOW IN A POROUS ATHEROSCLEROTIC MICROCHANNEL WITH THE PRESENCE OF A MAGNETIC FIELD, GROWTH RATE AND TREATMENT

K. W. Bunonyo

MMDARG, Department of Mathematics and Statistics, Federal University Otuoke, Nigeria

L. Ebiwareme

Department of Mathematics, Rivers State University, Port Harcourt, Nigeria

Abstract

Mathematical models representing blood flow through a microchannel with the effect of radiation-Brinkman number with an external magnetic field were formulated. The atherosclerosis is due to an exponential growth of cholesterol in the blood and trans fat consumption. The geometry of atherosclerosis was assumed to be growth rate and time dependent. The blood flow is considered nonlinear, incompressible, viscous, and fully developed. The nonlinear equations under suitable boundary conditions were scaled to a system of dimensionless PDE, which were reduced further to ordinary differential equations using the perturbation conditions. The perturbed system of ordinary differential equations was solved using the Laplace method. The blood flow profiles, such as velocity, volumetric flow rate, lipid concentration profiles such as lipid concentration and rate of mass of the lipid transfer, and temperature profiles such as blood temperature and the rate of heat transfer are obtained and the effects of the pertinent parameters such as magnetic field, radiation absorption, and Brinkman Number were discussed.

ARTICLEINFO

Article history:
Received 27 may 2022
Revised form 24 june 2022
Accepted 26 july 2022

Keywords: *Radiation, Brinkman Number, Blood, Atherosclerosis, Magnetic Field, Growth Rate, Treatment, Microchannel.*

---***---

The results show that the velocity increases with an increase in Brinkman number, Grashof number, solutal Grashof number and the porosity, while it decreases with an increase in Schmidt number, Prandtl number, radiation absorption, chemical reaction, and magnetic field. From the investigation, we could deduce that there is an increase in blood temperature with the increase in Brinkman number and a decrease in temperature due to an increase in Schmidt number, Prandtl number, radiation absorption, chemical reaction, and oscillatory frequency. In conclusion, we have been able to formulate a mathematical representation of blood flow through a sclerotic microchannel, obtained an exact solution to the problem, and presented results that might be useful for mathematicians and clinicians.

1 Introduction

Blood, the heart, and blood vessels are all part of the cardiovascular system. Blood is essential because it serves as a transport agent in the human body. Unfortunately, plaques in human blood vessels such as arteries and capillaries can disrupt normal blood flow, leading to cardiovascular diseases such as heart attack and stroke. Because of the implications for medicine and fluid mechanics, abnormal blood flow has piqued the interest of many researchers. Blood can be classified as a non-Newtonian fluid, so studies that involve modeling blood flow should take this into account. Humans are constantly confronted with challenges that disrupt the normal circulation of blood. This includes, among other things, physical exercises, vehicle travel, and application, according to Bunonyo *et al.* [1].

Over the years, lots of mathematicians and scientists have done ample research on the flow of blood in the human circulatory system and have discovered some useful results; here are a few of those studies supporting this research work. Bunonyo *et al.* [2] studied the impact of treatment parameters on blood flow in an atherosclerotic artery. Bhatti *et al.* [3] investigated the heat transfer analysis of peristaltic induced motion of particle fluid suspension with variable viscosity: the clot blood model. The influence of blood flow in large vessels on temperature distribution in hyperthermia was analyzed by Lagendijk [4]. Srivastava [5] discussed the analysis of the flow characteristics of blood flowing through an inclined tapered porous artery with mild stenosis under the influence of an inclined magnetic field. Bunonyo and Amos [6] investigated the effects of treatment and radiation on oscillatory blood flow through a stenosed artery. The study of slip effects on the unsteady MHD pulsating blood flow through a porous medium in an artery under the effect of body acceleration was carried out by Eldesoky [7]. Makinde and Mhone [8] investigated the heat transfer to MHD oscillatory flow in a channel filled with porous medium. Unsteady heat transfer to oscillatory flow through a porous medium under a slip condition was explained by Hamza *et al.* [9]. Choudhury and Das [10] studied the heat transfer to MHD oscillatory viscoelastic flow in a channel filled with porous medium. Biswas and Chakraborty [11] gave the pulsatile flow of blood in a constricted artery with body acceleration. Hanvey *et al.* [12] developed a model of heat and mass transfer in the oscillatory flow of a non-Newtonian fluid between two inclined porous plates placed in a magnetic field. Plourde *et al.* [13] looked into alterations in blood flow through arteries following atherectomy and the impact on pressure variation and velocity. Mathematical modeling of blood flow through vertebral arteries with stenosis was studied by Ali *et al.* [14]. Mathur and Jain [15] discussed the mathematical model of non-Newtonian blood flow through an artery in the presence of stenosis. Ali and Asghar [16] studied the oscillation channel flow for non-Newtonian fluids.

Varshney, Katiyar, and Kumar [17] investigated the effect of a magnetic field on the blood flow in an artery having multiple stenosis. Elangovan and Selvaraj [18] gave an insight into multiple stenosed arteries with periodic body acceleration in the presence of a magnetic field. Transport of MHD couple stress fluid through peristalsis in a porous medium under the influence of heat transfer and slip effects was investigated by Sankad and Nagathan [19]. Tripathi and Sharma [20] studied the effects of variable viscosity on MHD inclined arterial blood flow with chemical reaction. Modeling of arterial stenosis and its applications to blood flow was given by Pralhad and Schultz [21]. Bunonyo and Amadi [22] investigated the oscillatory flow of an electo-hydrodynamic fluid flow through a channel with a radiative heat and magnetic field.

Bunonyo and Eli [23] investigated the convective fluid flow through a sclerotic oscillatory artery in the presence of radiative heat and a magnetic field.

In this research, radiation-brinkman number effects on blood flow in a porous atherosclerotic microchannel with the presence of a magnetic field, growth rate, and treatment are investigated using the Laplace method. It involves the use of mathematical models to represent blood momentum in an arterial channel, flowing through an atherosclerotic artery due to an exponential growth of cholesterol on the upper walls of the artery. The simulated results are presented graphically by investigating the varying pertinent parameters.

2 Models Formulation

We consider blood to be unsteady, electrically conducting, and incompressible viscous blood flowing through an atherosclerotic artery, which is presumed to be a cylindrical microchannel with a velocity $w^*\left(r^*, x^*\right)$, where r^* and x^* the directions of the flow. The flow in the azimuthal direction is considered to be zero. The flow is due to the pumping action of the heart; the pressure gradient is in the horizontal direction; and the magnetic field is perpendicularly applied to the direction of the flow of blood. The models governing the flow can be presented as:

2.1 The geometry of atherosclerosis

$$R = \begin{cases} R_0 - \dfrac{\delta^*}{2}\left(1 + cos\dfrac{2\pi x^*}{\lambda^*}\right) & \text{at } d_0 \le x^* \le \lambda^* \\ R_0 & \text{at } 0 \le x^* \le d_0 \end{cases} \tag{1}$$

where $x^* = \left(d_0 + \dfrac{\lambda^*}{2}\right)$ (2)

2.2 Blood Momentum Equation

$$\rho_b \frac{\partial w^*}{\partial t^*} = -\frac{\partial P^*}{\partial x^*} + \mu_b\left(\frac{\partial^2 w^*}{\partial r^{*2}} + \frac{1}{r^*}\frac{\partial w^*}{\partial r^*}\right) - \frac{\mu_b \varphi}{k^*} w^* - \sigma B_0^2 w^* + \rho_b g \beta_T\left(T^* - T_\infty\right) + \rho_b g \beta_C\left(C^* - C_\infty\right) \tag{3}$$

2.3 Energy Equation

$$\rho_b c_b \frac{\partial T^*}{\partial t^*} = k_{Tb}\left(\frac{\partial^2 T^*}{\partial r^{*2}} + \frac{1}{r^*}\frac{\partial T^*}{\partial r^*}\right) - Q_0\left(T^* - T_\infty\right) + Q_1^*\left(C^* - C_\infty\right) \tag{4}$$

2.4 Lipid Concentration Equation

$$\frac{\partial C^*}{\partial t^*} = D_m\left(\frac{\partial^2 C^*}{\partial r^{*2}} + \frac{1}{r^*}\frac{\partial C^*}{\partial r^*}\right) - k_0\left(C^* - C_\infty\right) \tag{5}$$

The corresponding boundary conditions are

$$\left.\begin{aligned} & w^* = 0, T^* = T_w, C^* = C_w \quad \text{at } r^* = R \\ & w^* \ne 0, T^* \ne T_\infty, C^* \ne C_\infty \quad \text{at } r^* = 0 \end{aligned}\right\} \tag{6}$$

2.5 Dimensionless Scaling Parameters

$$\left.\begin{aligned}
&x=\frac{x^*}{\lambda^*},r=\frac{r^*}{R_0},t=\frac{t^*\upsilon_b}{R_0^2},w=\frac{w^*R_0}{\upsilon_b},Gr=\frac{g\beta_T\left(T_w-T_\infty\right)R_0^3}{\upsilon_b^2},\theta=\frac{T^*-T_\infty}{T_w-T_\infty},Rd_3=\frac{k_0R_0^2}{\upsilon_b}\\
&S_r=\frac{D_Tk_{Tb}}{\upsilon_bT_m}\left(\frac{T_w-T_\infty}{C_w-C_\infty}\right),Rd_1=\frac{Q_0R_0^2}{\mu_bc_b},Rd_2=\frac{Q_1R_0^2\left(C_w-C_\infty\right)}{k_{Tb}\left(T_w-T_\infty\right)},Gc=\frac{g\beta_C\left(C_w-C_\infty\right)R_0^3}{\upsilon_b^2},\\
&M=B_0R_0\sqrt{\frac{\sigma}{\mu_b}},\frac{1}{k}=\frac{\varphi R_0^2}{k^*},Sc=\frac{\upsilon_b}{D_m},\delta^*=\frac{\delta R_Te^{at}}{R_0},Pr=\frac{\mu_bc_b}{k_{Tb}},P=\frac{R_0^3P^*}{\lambda^*\mu_b\upsilon_b},\phi=\frac{C^*-C_\infty}{C_w-C_\infty},\\
&Q_1^*=\frac{\rho_bw^{*2}}{\upsilon_b\left(C_w-C_\infty\right)},Br=\frac{\mu_bw^2}{k_{Tb}\left(T_w-T_\infty\right)},\frac{\delta}{R_0}\ll 1
\end{aligned}\right\}\tag{7}$$

Applying the Dimensionless parameters in equation (7), equations (1)-(6) are reduced to

$$\frac{R}{R_0}=\begin{cases}1-\dfrac{R_T}{2}e^{at}\left(1+cos2\pi x\right) & \text{at } d_0\le x^*\le\lambda^*\\ 1 & \text{at } 0\le x^*\le d_0\end{cases}\tag{8}$$

$$\text{where } x=\frac{1}{\lambda}\left(d_0+\frac{\lambda}{2}\right)\tag{9}$$

$$\frac{\partial w}{\partial t}=-\frac{\partial P}{\partial x}+\left(\frac{\partial^2w}{\partial r^2}+\frac{1}{r}\frac{\partial w}{\partial r}\right)-\frac{1}{k}w-M^2w+Gr\theta+Gc\phi\tag{10}$$

$$Pr\frac{\partial\theta}{\partial t}=\left(\frac{\partial^2\theta}{\partial r^2}+\frac{1}{r}\frac{\partial\theta}{\partial r}\right)-Rd_1Pr\theta+Br\phi\tag{11}$$

$$Sc\frac{\partial\phi}{\partial t}=\left(\frac{\partial^2\phi}{\partial r^2}+\frac{1}{r}\frac{\partial\phi}{\partial r}\right)-Rd_3Sc\phi\tag{12}$$

The corresponding boundary conditions are

$$\left.\begin{aligned}&w\ne0,\theta\ne0,\phi\ne0\ \text{ at }\ r=0\\ &w=0,\theta=1,\phi=1\ \text{ at }\ r=\frac{R}{R_0}\end{aligned}\right\}\tag{13}$$

3 Reduction to ODE by Perturbation Method

We shall apply the perturbation method to reduce the partial differential equations (10)-(12) to ordinary differential equation, whence we can apply the appropriate method to solve the ODE. The solution to the PDE can be presented in the following form:

$$\left.\begin{aligned}&w(r,t)=w_0(r)e^{i\omega t}\\ &\theta(r,t)=\theta_0(r)e^{i\omega t}\\ &\phi(r,t)=\phi_0(r)e^{i\omega t}\\ &-\frac{\partial P}{\partial x}=P_0e^{i\omega t}\end{aligned}\right\}\tag{14}$$

Using equation (14) in reducing the PDE, we have the ODEs as follows:

$$\frac{d^2w_0}{dr^2}+\frac{1}{r}\frac{dw_0}{dr}-\beta_1^2w_0=-P_0-Gr\theta_0-Gc\phi_0 \tag{15}$$

$$\frac{d^2\theta_0}{dr^2}+\frac{1}{r}\frac{d\theta_0}{dr}-\beta_2^2\theta_0=-Br\phi_0 \tag{16}$$

$$\frac{d^2\phi_0}{dr^2}+\frac{1}{r}\frac{d\phi_0}{dr}-\beta_3^2\phi_0=0 \tag{17}$$

where $\beta_1^2=\left(\frac{1}{k}+M^2+i\omega\right), \beta_2^2=\left(Rd_1+i\omega\right)Pr, \beta_3^2=\left(Rd_3+i\omega\right)Sc$

The corresponding boundary conditions are

$$\left.\begin{array}{ll} w_0\neq 0, \theta_0\neq 0, \phi_0\neq 0 & \text{at } r=0 \\ w_0=0, \theta_0=e^{-i\omega t}, \phi_0=e^{-i\omega t} & \text{at } r=\frac{R}{R_0} \end{array}\right\} \tag{18}$$

4 Method of Solution

The Laplace of the basic function can be stated as follows:

$$L\{w_0(r)\}=w_0(s)=\int_0^\infty w_0(r)e^{-rs}dr \tag{19a}$$

$$L\{\theta_0(r)\}=\theta_0(s)=\int_0^\infty \theta_0(r)e^{-rs}dr \tag{19b}$$

$$L\{\phi_0(r)\}=\phi_0(s)=\int_0^\infty \phi_0(r)e^{-rs}dr \tag{19c}$$

Restating equation (17), we have

$$\frac{d^2\phi_0}{dr^2}+\frac{1}{r}\frac{d\phi_0}{dr}+\left(i\beta_3\right)^2\phi_0=0 \tag{19d}$$

We let $\beta_{31}=i\beta_3$, and then equation (19d) reduces to:

$$\frac{d^2\phi_0}{dr^2}+\frac{1}{r}\frac{d\phi_0}{dr}+\beta_{31}^2\phi_0=0 \tag{20}$$

Applying Laplace method in solving equation (20), we state it as follows

$$L\left\{r\frac{d^2\phi_0}{dr^2}\right\}+L\left\{\frac{d\phi_0}{dr}\right\}+\beta_{31}^2L\{r\phi_0\}=0 \tag{21}$$

Simplifying equation (21), we have

$$L\left\{r\frac{d^2\phi_0}{dr^2}\right\}+L\left\{\frac{d\phi_0}{dr}\right\}+\beta_{31}^2L\{r\phi_0\}=0=-\frac{d}{ds}\left(s^2\phi_0(s)-s\phi_0(0)-\dot{\phi}_0(0)\right)+s\phi_0(s)-\theta_0(0)-\beta_{31}^2\frac{d\phi_0}{ds} \tag{22}$$

$$\Rightarrow -\frac{d}{ds}\left(s^2\phi_0(s)-s\phi_0(0)-\dot{\phi}_0(0)\right)+s\phi_0(s)-\theta_0(0)-\beta_{31}^2\frac{d\phi_0}{ds}=0 \tag{23}$$

$$\Rightarrow \frac{d\phi_0}{ds} + \frac{s\phi_0}{\left(s^2+\beta_{31}^2\right)} = 0 \tag{24}$$

Simplifying equation (24), we have

$$\phi_0(s) = \frac{B_1}{\sqrt{\left(s^2+\beta_{31}^2\right)}} \tag{25}$$

Taking the inverse transform of equation (25), we have

$$\phi_0(r) = L^{-1}\left\{\frac{B_1}{\sqrt{\left(s^2+\beta_{31}^2\right)}}\right\} = B_1 J_0\left(\beta_{31} r\right) = B_1 J_0\left(i\beta_3 r\right) \tag{26}$$

Note that $J_0\left(i\beta_3 r\right) = I_0\left(\beta_3 r\right)$, so that equation (26) becomes

$$\phi_0(r) = B_1 I_0\left(\beta_3 r\right) \tag{27}$$

Solving for the constant coefficient in equation (27) using the condition in equation (18), we have

$$B_1 = \frac{e^{-i\omega t}}{I_0\left(\beta_3 h\right)} \tag{28}$$

Substituting equation (28) into equation (27), we have

$$\phi_0(r) = \left(\frac{e^{-i\omega t}}{I_0\left(\beta_3 h\right)}\right) I_0\left(\beta_3 r\right) \tag{29}$$

To obtain the lipid concentration profile, we shall substitute equation (29) into equation (14), which is

$$\phi(r,t) = \left(\frac{I_0\left(\beta_3 r\right)}{I_0\left(\beta_3 h\right)}\right) \tag{30}$$

Retransforming equation (16), we have

$$\frac{d^2\theta_0}{dr^2} + \frac{1}{r}\frac{d\theta_0}{dr} + \left(i\beta_2\right)^2 \theta_0 = -Br\phi_0 \tag{31}$$

We let $\beta_{21} = i\beta_2$, and then equation (31) reduces to:

$$\frac{d^2\theta_0}{dr^2} + \frac{1}{r}\frac{d\theta_0}{dr} + \beta_{21}^2 \theta_0 = -Br\phi_0 \tag{32}$$

Decompose equation (32) into homogenous and non-homogenous, which is

$$\frac{d^2\theta_0}{dr^2} + \frac{1}{r}\frac{d\theta_0}{dr} + \beta_{21}^2 \theta_0 = 0 \tag{33}$$

Solve equation (33) using Laplace method, which is

$$L\left\{r\frac{d^2\theta_0}{dr^2}\right\} + L\left\{\frac{d\theta_0}{dr}\right\} + \beta_{21}^2 L\left\{r\theta_0\right\} = 0 \tag{34}$$

Simplifying equation (34), we have

$$L\left\{r\frac{d^2\theta_0}{dr^2}\right\}+L\left\{\frac{d\theta_0}{dr}\right\}+\beta_{21}^2L\{r\theta_0\}=0=-\frac{d}{ds}\left(s^2\theta_0(s)-s\theta_0(0)-\dot{\theta}_0(0)\right)+s\theta_0(s)-\theta_0(0)-\beta_{21}^2\frac{d\theta_0}{ds} \tag{35}$$

Simplifying equation (35), we have

$$\frac{d\theta_0}{ds}+\frac{s}{\left(s^2+\beta_{21}^2\right)}\theta_0(s)=0 \tag{36}$$

Solving equation (36), we have

$$\theta_0(s)=\frac{B_2}{\sqrt{\left(s^2+\beta_{21}^2\right)}} \tag{37}$$

Taking the inverse transform of equation (37), we have:

$$\theta_0(r)=L^{-1}\left\{\frac{B_2}{\sqrt{\left(s^2+\beta_{21}^2\right)}}\right\}=B_2L^{-1}\left\{\frac{1}{\sqrt{\left(s^2+\beta_{21}^2\right)}}\right\}=B_2J_0(\beta_{21}r)=B_2J_0(i\beta_2r) \tag{38}$$

Note that $J_0(i\beta_2r)=I_0(\beta_2r)$, so that the homogenous solution of equation (32) is

$$\theta_0(r)=B_2I_0(\beta_2r) \tag{39}$$

Recalling equation (16) after substituting the lipid concentration profile, we have

$$\frac{d^2\theta_0}{dr^2}+\frac{1}{r}\frac{d\theta_0}{dr}-\beta_2^2\theta_0=-Br\left(\frac{e^{-i\omega t}}{I_0(\beta_3h)}\right)I_0(\beta_3r) \tag{40}$$

Let the particular solution be in the form

$$\theta_{0p}(r)=A_1+A_2I_0(\beta_3r) \tag{41}$$

Differentiate equation (41) twice according to the order of equation (40), which is

$$\frac{d\theta_{0p}}{dr}=A_2\beta_3I_1(\beta_3r),\frac{d^2\theta_{0p}}{dr^2}=A_2\beta_3^2I_1'(\beta_3r) \tag{42}$$

Substitute equations (42) and (41) into equation (40), we have

$$A_2\beta_3^2I_1^2(\beta_3r)+\frac{1}{r}\left(A_2\beta_3I_1(\beta_3r)\right)-\beta_2^2A_1-\beta_2^2A_2I_0(\beta_3r)=-Br\left(\frac{e^{-i\omega t}}{I_0(\beta_3h)}\right)I_0(\beta_3r) \tag{43}$$

Simplifying equation (43) we have

$$A_1=0,A_2=\frac{Br}{\beta_2^2}\left(\frac{e^{-i\omega t}}{I_0(\beta_3h)}\right) \tag{44}$$

Substitute equation (44) into equation (41), we have

$$\theta_{0p}(r)=\frac{Br}{\beta_2^2}\left(\frac{e^{-i\omega t}}{I_0(\beta_3h)}\right)I_0(\beta_3r) \tag{45}$$

The general solution of equation (16) is the sum of equations (45) and (39), which is

$$\theta_0(r) = B_2 I_0(\beta_2 r) + \frac{Br}{\beta_2^2}\left(\frac{e^{-i\omega t}}{I_0(\beta_3 h)}\right) I_0(\beta_3 r) \tag{46}$$

Solving equation (46) using the boundary condition in equation (18), we have

$$B_2 = \frac{e^{-i\omega t}}{I_0(\beta_2 h)} - \frac{Bre^{-i\omega t}}{\beta_2^2 I_0(\beta_2 h)} \tag{47}$$

Substitute equation (47) into equation (46), which is

$$\theta_0(r) = \left(\frac{e^{-i\omega t}}{I_0(\beta_2 h)} - \frac{Bre^{-i\omega t}}{\beta_2^2 I_0(\beta_2 h)}\right) I_0(\beta_2 r) + \frac{Br}{\beta_2^2}\left(\frac{e^{-i\omega t}}{I_0(\beta_3 h)}\right) I_0(\beta_3 r) \tag{48}$$

The temperature profile with the effect of the lipid concentration, we substitute equation (48) into equation (14), we have

$$\theta(r,t) = \left(\left(\frac{e^{-i\omega t}}{I_0(\beta_2 h)} - \frac{Bre^{-i\omega t}}{\beta_2^2 I_0(\beta_2 h)}\right) I_0(\beta_2 r) + \frac{Br}{\beta_2^2}\left(\frac{e^{-i\omega t}}{I_0(\beta_3 h)}\right) I_0(\beta_3 r)\right) e^{i\omega t} \tag{49}$$

The other key objectives of this research are to investigate impact of temperature and lipid concentration profiles on blood momentum. Let us recall the momentum equation as

$$\frac{d^2 w_0}{dr^2} + \frac{1}{r}\frac{dw_0}{dr} - \beta_1^2 w_0 = P_0 - Gr\theta_0 - Gc\phi_0 \tag{50}$$

Substitute equation (48) and (29) into equation (15), which is

$$\frac{d^2 w_0}{dr^2} + \frac{1}{r}\frac{dw_0}{dr} - \beta_1^2 w_0 = P_0 - \frac{Gre^{-i\omega t}}{I_0(\beta_2 h)}\left(1 - \frac{Br}{\beta_2^2}\right) I_0(\beta_2 r) - \left(\frac{e^{-i\omega t}}{I_0(\beta_3 h)}\right)\left(Gc + \frac{BrGr}{\beta_2^2}\right) I_0(\beta_3 r) \tag{51}$$

To solve the homogenous part of equation (51), we let it to be equal to zero, that is

$$\frac{d^2 w_0}{dr^2} + \frac{1}{r}\frac{dw_0}{dr} - \beta_1^2 w_0 = 0 \tag{52}$$

We can further transform equation (52) as

$$\frac{d^2 w_0}{dr^2} + \frac{1}{r}\frac{dw_0}{dr} + (i\beta_1)^2 w_0 = 0 \tag{53}$$

We let $\beta_{11} = i\beta_1$, and then equation (53) reduces to:

$$\frac{d^2 w_0}{dr^2} + \frac{1}{r}\frac{dw_0}{dr} + \beta_{11}^2 w_0 = 0 \tag{54}$$

Solve equation (54) using Laplace method, which is

$$L\left\{r\frac{d^2 w_0}{dr^2}\right\} + L\left\{\frac{dw_0}{dr}\right\} + \beta_{11}^2 L\{rw_0\} = 0 \tag{55}$$

Simplifying equation (55), we have

$$L\left\{r\frac{d^2w_0}{dr^2}\right\}+L\left\{\frac{dw_0}{dr}\right\}+\beta_{11}^2L\{rw_0\}=0=-\frac{d}{ds}\left(s^2w_0(s)-sw_0(0)-\dot{\theta}_0(0)\right)+sw_0(s)-w_0(0)-\beta_{11}^2\frac{dw_0}{ds} \tag{56}$$

Simplifying equation (56), we have

$$\frac{dw_0}{ds}+\frac{s}{\left(s^2+\beta_{11}^2\right)}w_0(s)=0 \tag{57}$$

Solving equation (57), we have

$$w_0(s)=\frac{B_3}{\sqrt{\left(s^2+\beta_{11}^2\right)}} \tag{58}$$

Taking the inverse transform of equation (58), we have:

$$w_0(r)=L^{-1}\left\{\frac{B_3}{\sqrt{\left(s^2+\beta_{11}^2\right)}}\right\}=B_3L^{-1}\left\{\frac{1}{\sqrt{\left(s^2+\beta_{11}^2\right)}}\right\}=B_3J_0(\beta_{11}r)=B_3J_0(i\beta_1r) \tag{59}$$

Note that $J_0(i\beta_1r)=I_0(\beta_1r)$, so that equation (59) which is

$$w_0(r)=B_3I_0(\beta_1r) \tag{60}$$

Recalling equation (51) after substituting the lipid concentration profile, we have

$$\frac{d^2w_0}{dr^2}+\frac{1}{r}\frac{dw_0}{dr}-\beta_1^2w_0=P_0-\frac{Gre^{-i\omega t}}{I_0(\beta_2h)}\left(1-\frac{Br}{\beta_2^2}\right)I_0(\beta_2r)-\left(\frac{e^{-i\omega t}}{I_0(\beta_3h)}\right)\left(Gc+\frac{BrGr}{\beta_2^2}\right)I_0(\beta_3r) \tag{61}$$

The particular solution of equation (62) takes the form

$$w_{0p}(r)=A_4+A_5I_0(\beta_2r)+A_6I_0(\beta_3r) \tag{62}$$

Differentiate equation (62) twice according to the order of equation (61), which is

$$\frac{dw_{0p}}{dr}=\left(A_5\beta_2I_1(\beta_2r)+A_6\beta_3I_1(\beta_3r)\right),\ \frac{d^2w_{0p}}{dr^2}=\left(A_5\beta_2^2I_1'(\beta_2r)+A_6\beta_3^2I_1'(\beta_3r)\right) \tag{63}$$

Substitute equations (63) and (62) into equation (61) and solving, we have

$$A_4=\frac{P_0}{\beta_1^2},A_5=\frac{1}{\beta_1^2}\left(\frac{Gre^{-i\omega t}}{I_0(\beta_2h)}\left(1-\frac{Br}{\beta_2^2}\right)\right),A_6=\frac{1}{\beta_1^2}\left(Gc+\frac{BrGr}{\beta_2^2}\right)\left(\frac{e^{-i\omega t}}{I_0(\beta_3h)}\right) \tag{64}$$

Substitute equation (64) into equation (62), we have the particular solution as

$$w_{0p}(r)=\frac{P_0}{\beta_1^2}+\frac{1}{\beta_1^2}\left(\frac{Gre^{-i\omega t}}{I_0(\beta_2h)}\left(1-\frac{Br}{\beta_2^2}\right)\right)I_0(\beta_2r)+\frac{1}{\beta_1^2}\left(Gc+\frac{BrGr}{\beta_2^2}\right)\left(\frac{e^{-i\omega t}}{I_0(\beta_3h)}\right)I_0(\beta_3r) \tag{65}$$

The general solution of equation (62) is the sum of equations (65) and (60), which is

$$w_0(r)=B_3I_0(\beta_1 r)+\frac{P_0}{\beta_1^2}+\frac{1}{\beta_1^2}\left(\frac{Gre^{-i\omega t}}{I_0(\beta_2 h)}\left(1-\frac{Br}{\beta_2^2}\right)\right)I_0(\beta_2 r)+\frac{1}{\beta_1^2}\left(Gc+\frac{BrGr}{\beta_2^2}\right)\left(\frac{e^{-i\omega t}}{I_0(\beta_3 h)}\right)I_0(\beta_3 r) \tag{66}$$

$$w(r,t)=\left(B_3I_0(\beta_1 r)+\frac{P_0}{\beta_1^2}+\frac{1}{\beta_1^2}\left(\frac{Gre^{-i\omega t}}{I_0(\beta_2 h)}\left(1-\frac{Br}{\beta_2^2}\right)\right)I_0(\beta_2 r)+\frac{1}{\beta_1^2}\left(Gc+\frac{BrGr}{\beta_2^2}\right)\left(\frac{e^{-i\omega t}}{I_0(\beta_3 h)}\right)I_0(\beta_3 r)\right)e^{i\omega t} \tag{67}$$

where $B_3=\frac{Gre^{-i\omega t}}{\beta_1^2 I_0(\beta_1 h)}\left(\frac{Br}{\beta_2^2}-1\right)-\frac{P_0}{\beta_1^2 I_0(\beta_1 h)}-\frac{e^{-i\omega t}}{\beta_1^2 I_0(\beta_1 h)}\left(Gc+\frac{BrGr}{\beta_2^2}\right)$

The flow cab be calculated mathematically as

$$Q=2\pi e^{i\omega t}\int_{r=0}^{r=h} r\left(B_3I_0(\beta_1 r)+\frac{P_0}{\beta_1^2}+\frac{1}{\beta_1^2}\left(\frac{Gre^{-i\omega t}}{I_0(\beta_2 h)}\left(1-\frac{Br}{\beta_2^2}\right)\right)I_0(\beta_2 r)+\frac{1}{\beta_1^2}\left(Gc+\frac{BrGr}{\beta_2^2}\right)\left(\frac{e^{-i\omega t}}{I_0(\beta_3 h)}\right)I_0(\beta_3 r)\right)dr \tag{68}$$

Simplifying equation (68), we have

$$Q=2\pi e^{i\omega t}\left(\begin{array}{l}\int_{r=0}^{r=h} B_3 rI_0(\beta_1 r)\,dr+\int_{r=0}^{r=h}\frac{1}{\beta_1^2}\left(\frac{Gre^{-i\omega t}}{I_0(\beta_2 h)}\left(1-\frac{Br}{\beta_2^2}\right)\right)rI_0(\beta_2 r)\,dr\\ +\int_{r=0}^{r=h}\frac{1}{\beta_1^2}\left(Gc+\frac{BrGr}{\beta_2^2}\right)\left(\frac{e^{-i\omega t}}{I_0(\beta_3 h)}\right)rI_0(\beta_3 r)\,dr+\int_{r=0}^{r=h}\frac{P_0 r}{\beta_1^2}dr\end{array}\right) \tag{69}$$

After integration and substituting the limit of integration, we have

$$Q=2\pi e^{i\omega t}\left(\begin{array}{l}\frac{B_3 h}{\beta_1}I_1(\beta_1 h)+\frac{h}{\beta_2\beta_1^2}\left(\frac{Gre^{-i\omega t}}{I_0(\beta_2 h)}\left(1-\frac{Br}{\beta_2^2}\right)\right)I_1(\beta_2 h)+\\ \frac{h}{\beta_3\beta_1^2}\left(Gc+\frac{BrGr}{\beta_2^2}\right)\left(\frac{e^{-i\omega t}}{I_0(\beta_3 h)}\right)I_1(\beta_3 h)+\frac{P_0 h^2}{2\beta_1^2}\end{array}\right) \tag{70}$$

The rate of lipid transfer can be calculated mathematically as

$$Sh=-\left.\frac{\partial w}{\partial r}\right|_{r=h}=\frac{\partial}{\partial r}\left(\frac{I_0(\beta_3 r)}{I_0(\beta_3 h)}\right)_{r=h}=\frac{\beta_3 I_1(\beta_3 h)}{I_0(\beta_3 h)} \tag{71}$$

The rate of heat transfer can be calculated mathematically as

$$Nu=\left.\frac{\partial\theta}{\partial r}\right|_{r=h}=\left(\beta_2\left(\frac{e^{-i\omega t}}{I_0(\beta_2 h)}-\frac{Bre^{-i\omega t}}{\beta_2^2 I_0(\beta_2 h)}\right)I_1(\beta_2 h)+\frac{Br\beta_3}{\beta_2^2}\left(\frac{e^{-i\omega t}}{I_0(\beta_3 h)}\right)I_1(\beta_3 h)\right)e^{i\omega t} \tag{72}$$

5 Results

Numerical computations were performed using the data values presented below:

$R_T=04, \delta=0.4, a=0.35, x=0.3, 0\le Sc\le 10, 2\le Rd_1\le 10, 0.5\le Rd_3\le 3, 2.1\le Pr\le 21,$
$1\le Br\le 10, 1.5\le M\le 5, 2\le\omega\le 10, 0\le k\le 0.1, 5\le Gr\le 30, 5\le Gc\le 5.$

The results are presented in the following ways; Figs (1)-(3) represent the lipid concentration, Figs(4)-(6) representing the rate of mass transfer, Figs (7)-(12) representing the blood temperature profile, Figs(13)-(18) for rate of heat transfer, Figs(19)-(26) representing the blood velocity profile for different pertinent parameter values and finally, Figs (27)-(33) showing the blood volumetric flow rate for different pertinent parameters.

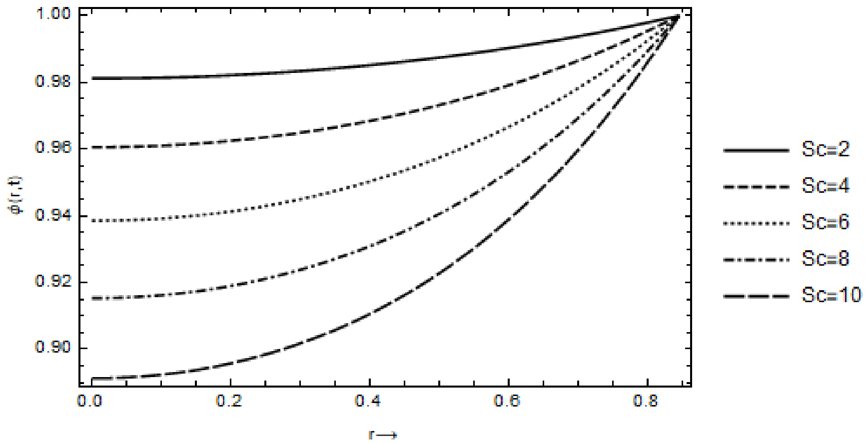

Fig 1 Effect on Schmidt number on Lipid Concentration with other values $Rd_3 = 0.5, \omega = 0.3, x = 0.3$

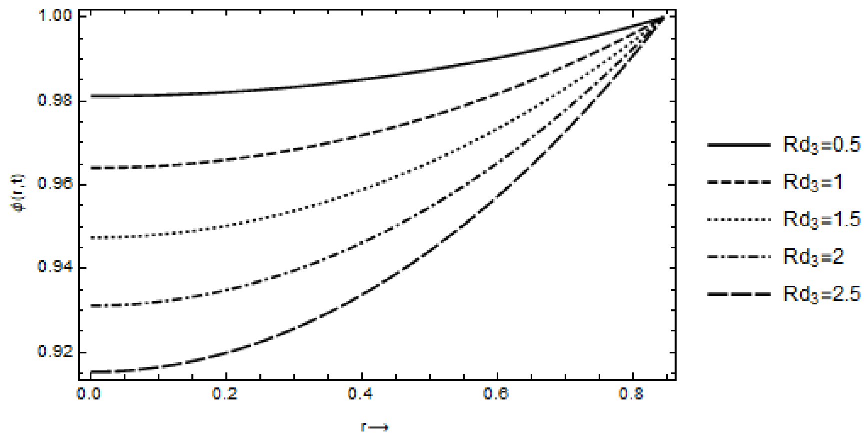

Fig 2 Effect on Chemical Reaction on Lipid Concentration with other values $Sc = 0.2, \omega = 0.3, x = 0.3$

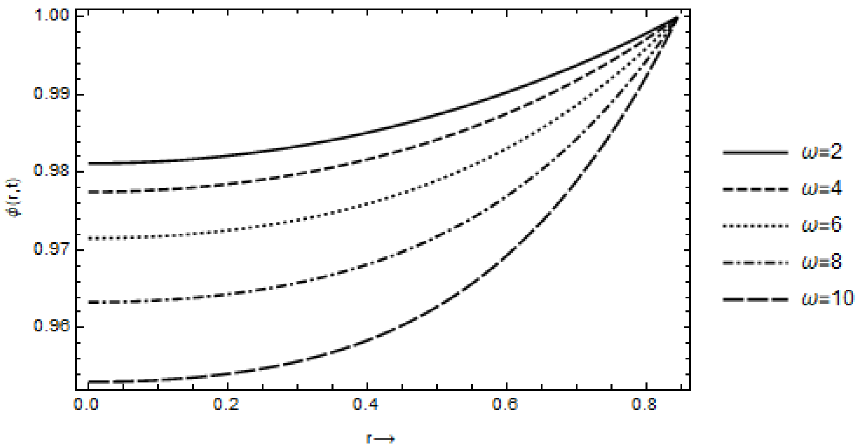

Fig 3 Effect of Oscillatory Frequency on Lipid Concentration with other values $Sc = 0.2, Rd_3 = 0.5, x = 0.3$

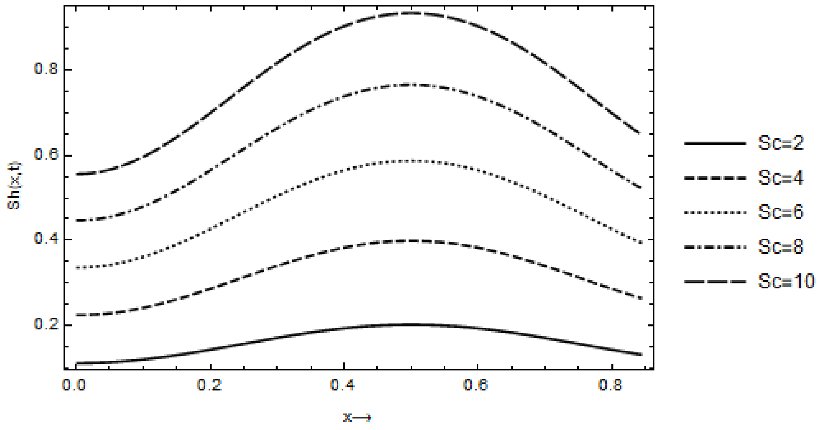

Fig 4 Effect of Schmidt Number on Rate of Mass Transfer with other values $Rd_3 = 0.5, \omega = 0.3$

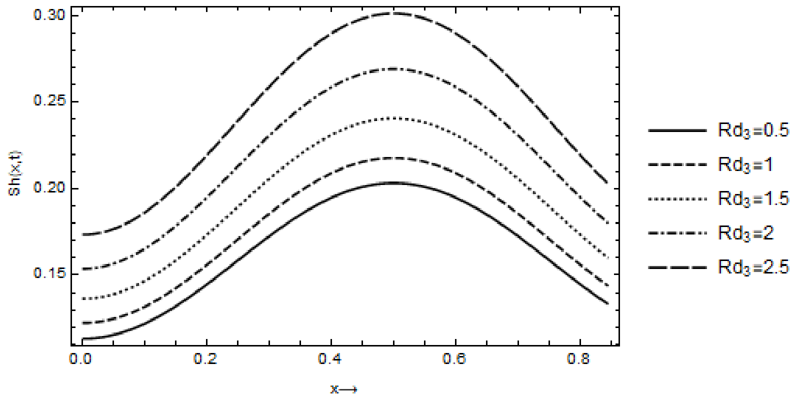

Fig 5 Effect of Chemical Reaction on Rate of Mass Transfer with other values $Sc = 0.2, \omega = 0.3$

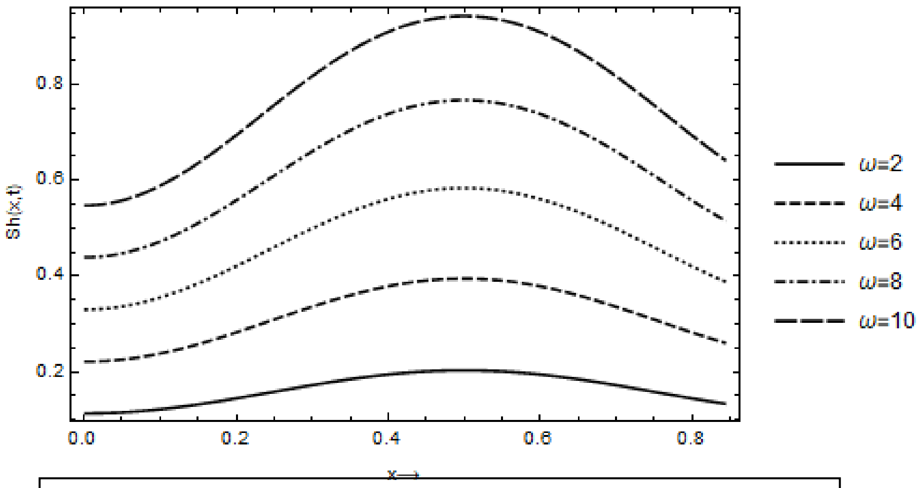

Fig 6 Effect of Oscillatory Frequency on Rate of Mass Transfer with other values $Sc = 0.2, Rd_3 = 0.5$

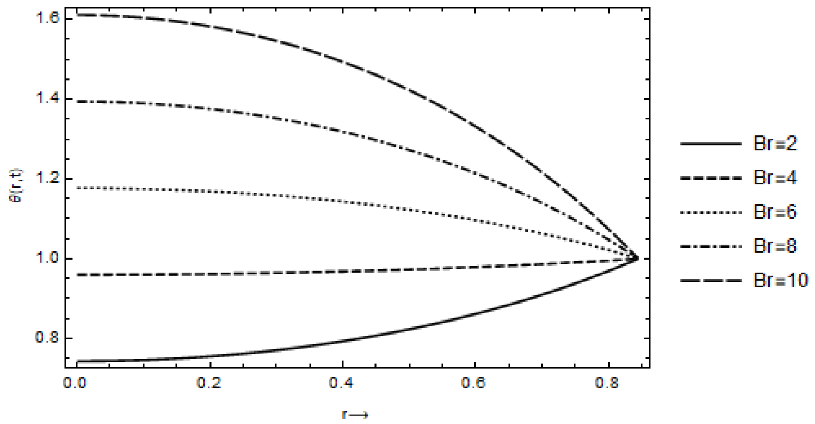

Fig 7 Effect of Brinkman Number on Blood Temperature other values $Sc = 0.2, \omega = 0.3, Pr = 2.1, Rd_1 = 2, Rd_3 = 0.3$

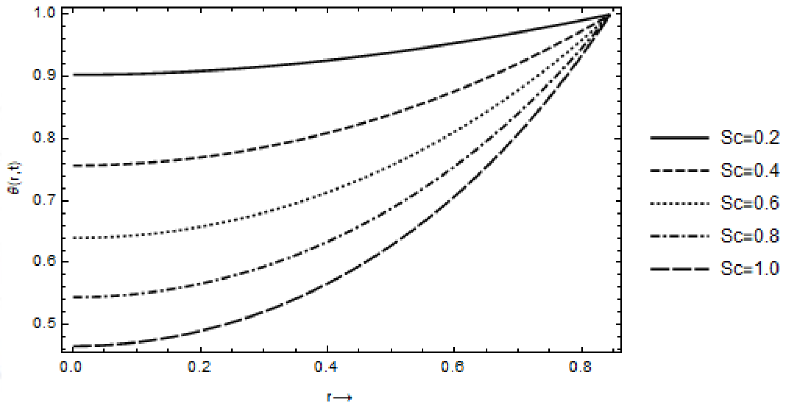

Fig 8 Effect of Schmidt Number on Blood Temperature with other values $Rd_3 = 0.3, \omega = 0.3, Pr = 2.1, Rd_1 = 2, Br = 5$

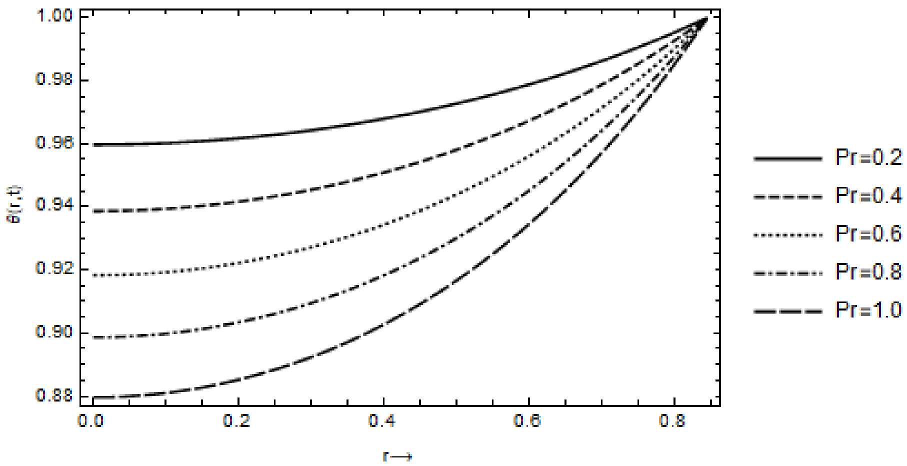

Fig 9 Effect of Prandtl Number on Blood Temperature with other values $Sc = 0.2, \omega = 0.3, Rd_3 = 0.3, Rd_1 = 2, Br = 5$

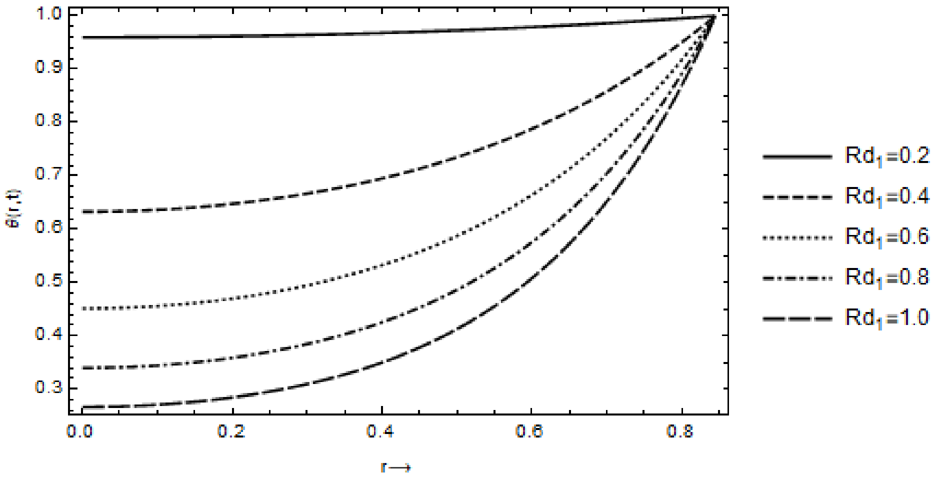

Fig 10 Effect of Radiation Absorption on Blood Temperature with other values $Sc = 0.2, \omega = 0.3, Pr = 2.1, Rd_3 = 0.3, Br = 5$

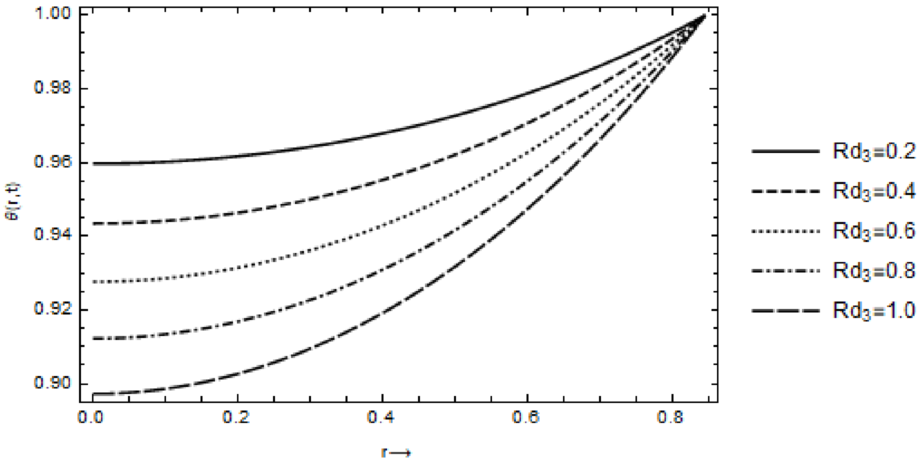

Fig 11 Effect of Chemical Reaction on Blood Temperature with other values $Sc = 0.2, \omega = 0.3, Pr = 2.1, Rd_1 = 2, Br = 5$

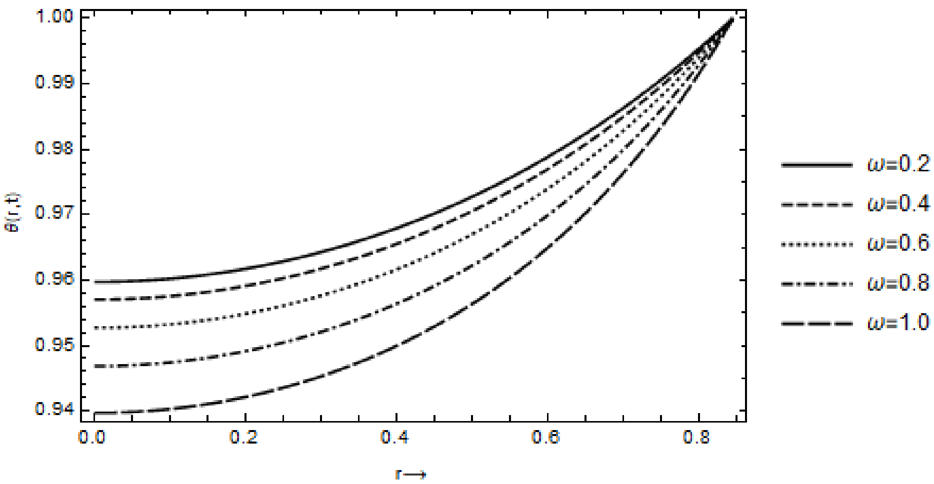

Fig 12 Effect of Oscillatory Frequency on Blood Temperature with other values $Sc = 0.2, Rd_3 = 0.3, Pr = 2.1, Rd_1 = 2, Br = 5$

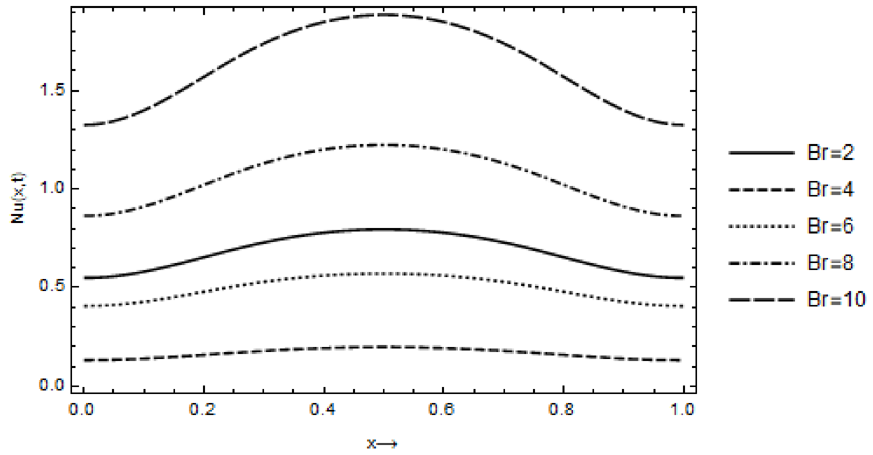

Fig 13 Effect of Brinkman number on Rate of Heat Transfer with other values $Sc = 0.2, \omega = 0.3, Pr = 2.1, Rd_1 = 2, Rd_3 = 0.3$

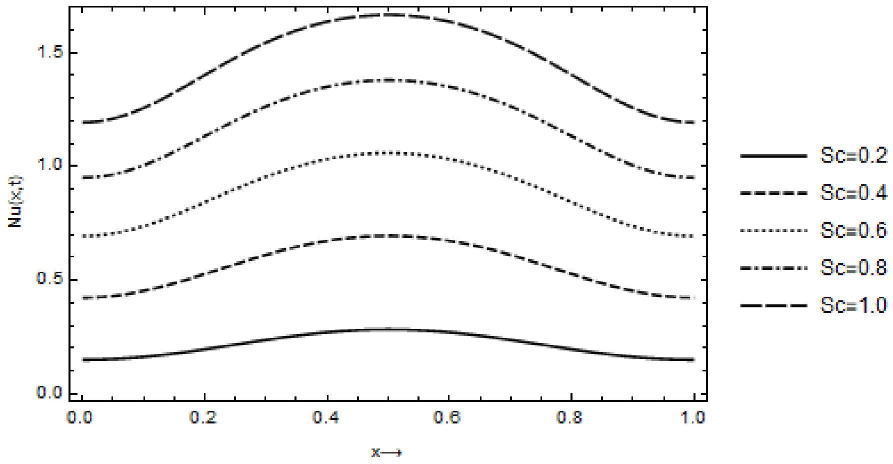

Fig 14 Effect of Schmidt Number on Rate of Heat Transfer with other values $Rd_3 = 0.3, \omega = 0.3, Pr = 2.1, Rd_1 = 2, Br = 5$

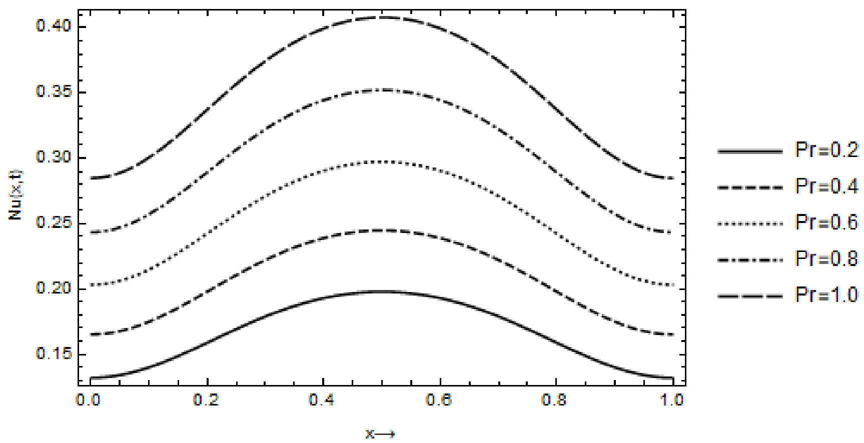

Fig 15 Effect of Prandtl Number on Rate of Heat Transfer with other values $Sc = 0.2, \omega = 0.3, Rd_3 = 0.3, Rd_1 = 2, Br = 5$

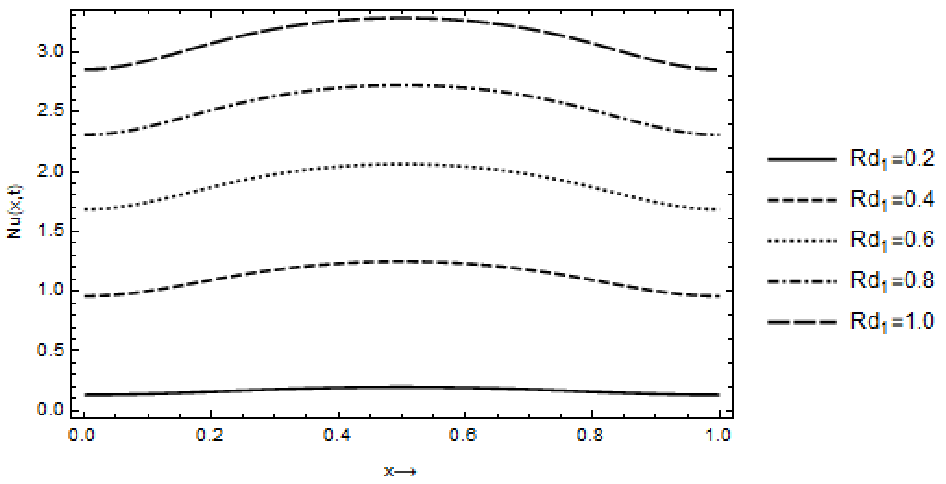

Fig 16 Effect of Radiation Absorption on Rate of Heat Transfer with other values $Sc = 0.2, \omega = 0.3, Pr = 2.1, Rd_3 = 0.3, Br = 5$

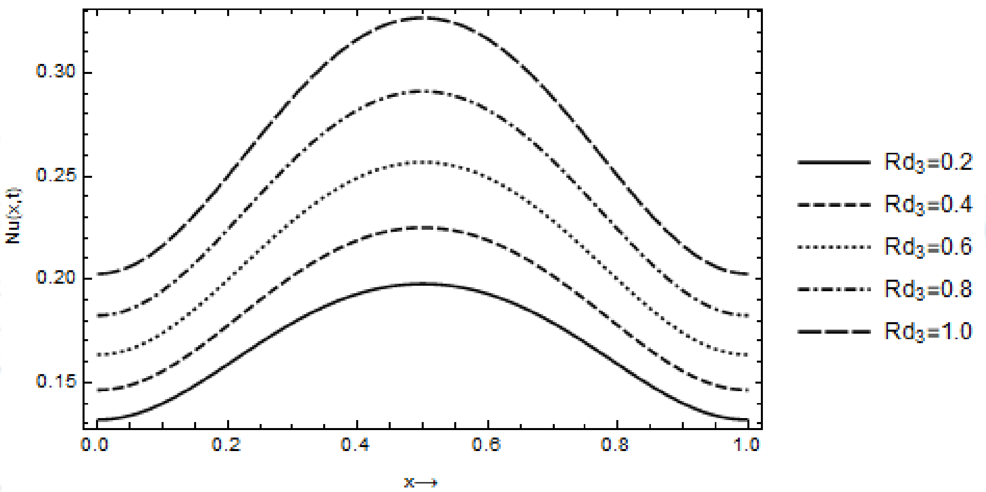

Fig 17 Effect of Chemical Reaction on Rate of Heat Transfer with other values $Sc = 0.2, \omega = 0.3, Pr = 2.1, Rd_1 = 2, Br = 5$

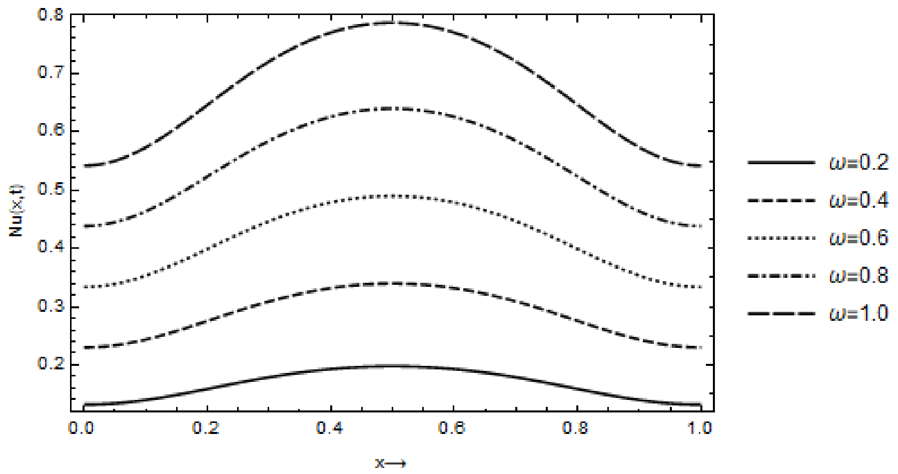

Fig 18 Effect of Oscillatory Frequency of Heat Transfer with other values $Sc = 0.2, Rd_3 = 0.3, Pr = 2.1, Rd_1 = 2, Br = 5$

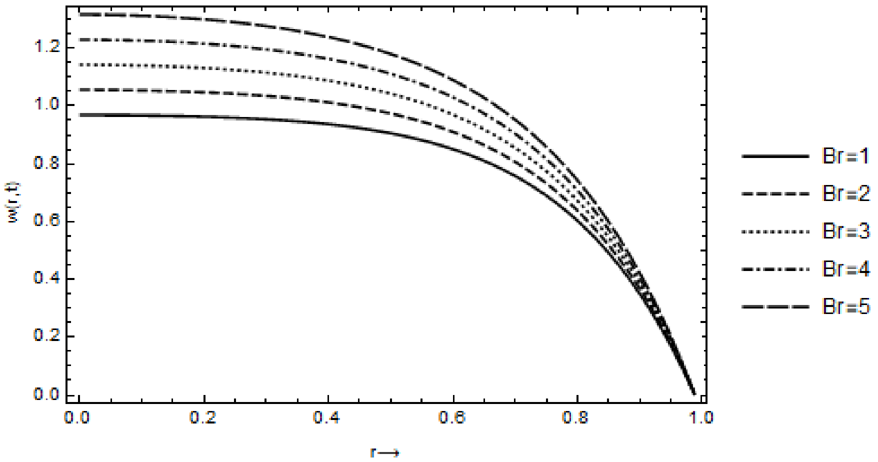

Fig 19 Effect of Brinkman number on Blood Velocity with other values $Gc = 15$, $Gr = 15, Pr = 2.1, Sc = 2, Rd_3 = 2, Rd_1 = 2, \omega = 0.3, k = 0.05, M = 1.5, x = 0.3$

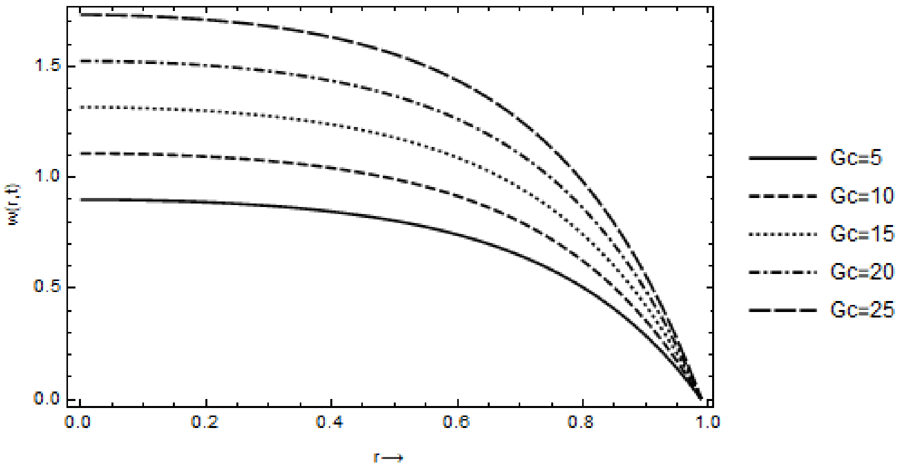

Fig 20 Effect of Solutal Grashof Number on Blood Velocity with other values $Br = 5, Gr = 15, Pr = 2.1, Sc = 2, Rd_3 = 2, Rd_1 = 2, \omega = 0.3, k = 0.05, M = 1.5, x = 0.3$

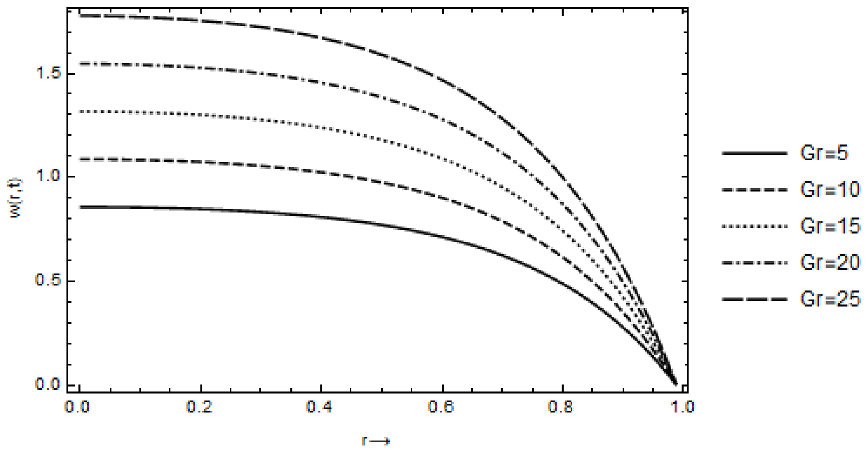

Fig 20 Effect of Grashof Number on Blood Velocity with other values $Br = 5$, $Gc = 15, Pr = 2.1, Sc = 2, Rd_3 = 2, Rd_1 = 2, \omega = 0.3, k = 0.05, M = 1.5, x = 0.3$

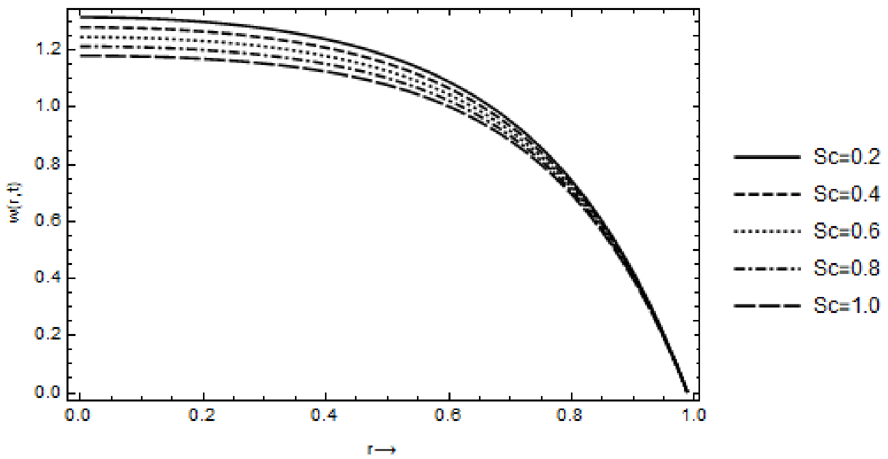

Fig 21 Effect of Schmidt Number on Blood Velocity with other values $Br = 5$, $Gc = 15, Gr = 15, Pr = 2.1, Rd_3 = 2, Rd_1 = 2, \omega = 0.3, k = 0.05, M = 1.5, x = 0.3$

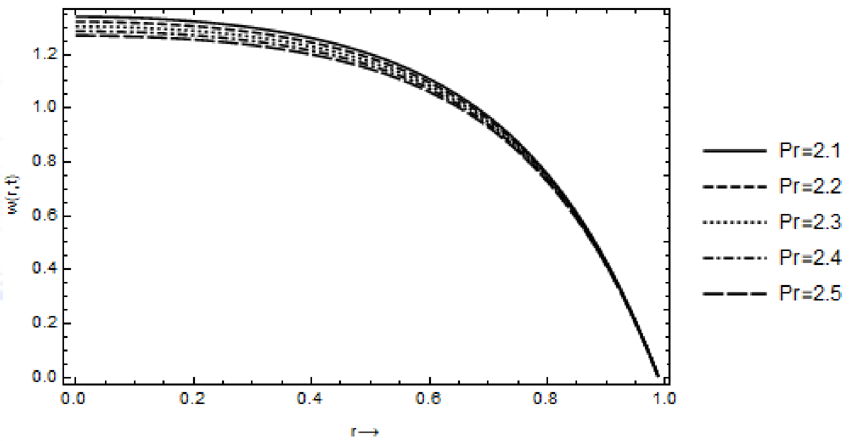

Fig 22 Effect of Prandtl Number on Blood Velocity with other value $Br = 5, Gc = 15$, $Gr = 15, Pr = 2.1, Sc = 2, Rd_3 = 2, Rd_1 = 2, \omega = 0.3, k = 0.05, M = 1.5, x = 0.3$

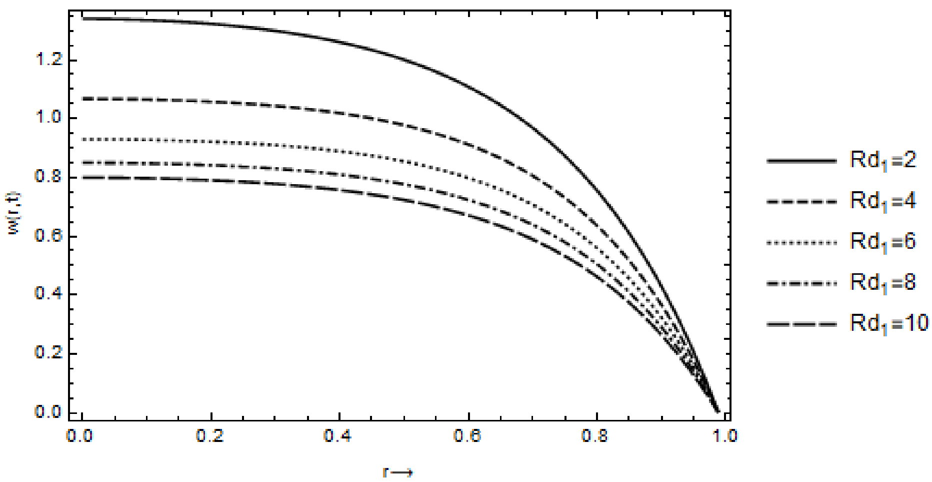

Fig 23 Effect of Radiation Absorption on Blood Velocity with other values $Br = 5$, $Gc = 15, Gr = 15, Pr = 2.1, Sc = 2, Rd_3 = 2, \omega = 0.3, k = 0.05, M = 1.5, x = 0.3$

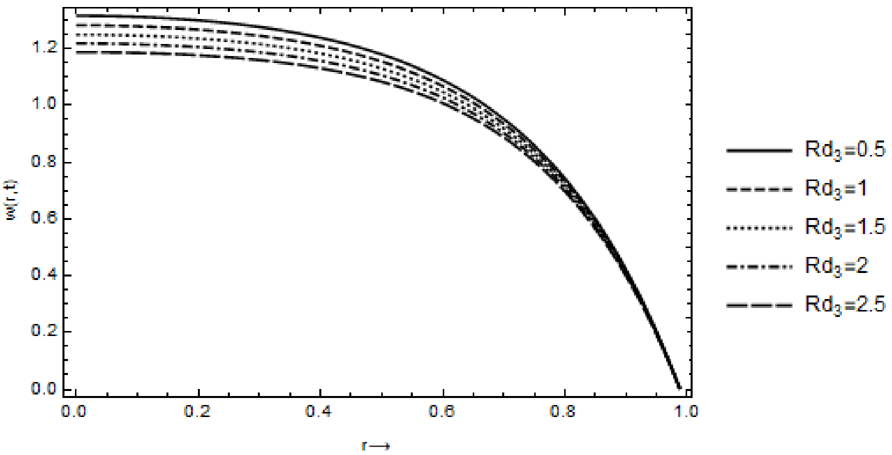

Fig 24 Effect of Chemical reaction on Blood Velocity with other value $Br = 5$, $Gc = 15, Gr = 15, Pr = 2.1, Sc = 2, Rd_1 = 2, \omega = 0.3, k = 0.05, M = 1.5, x = 0.3$

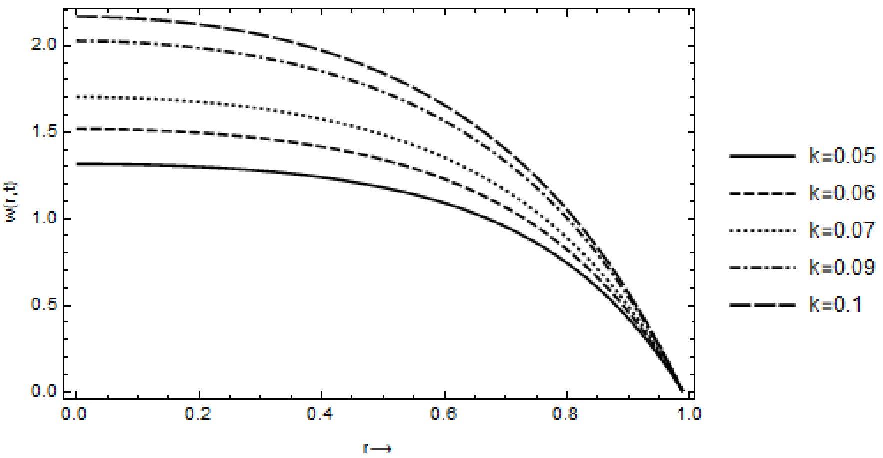

Fig 25 Effect of Porosity on Blood Velocity with other values $Br = 5, Gc = 15$, $Gr = 15, Pr = 2.1, Sc = 2, Rd_3 = 2, Rd_1 = 2, \omega = 0.3, M = 1.5, x = 0.3$

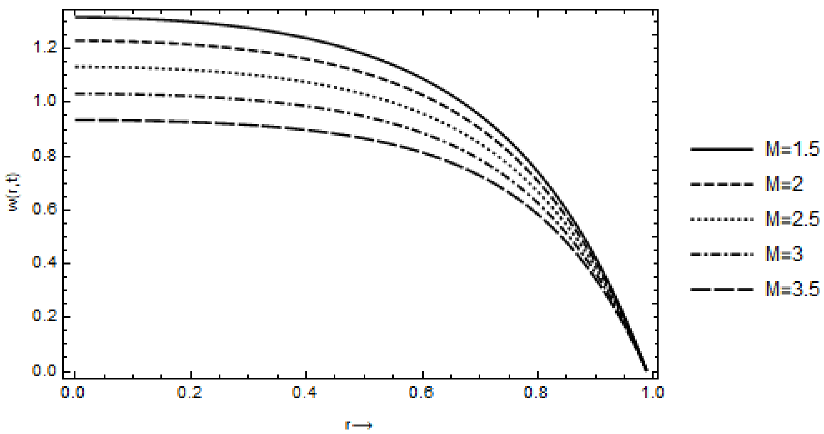

Fig 26 Effect of Magnetic Field on Blood Velocity with other values $Br = 5, Gc = 15, Gr = 15, Pr = 2.1, Sc = 2, Rd_3 = 2, Rd_1 = 2, \omega = 0.3, k = 0.05, x = 0.3$

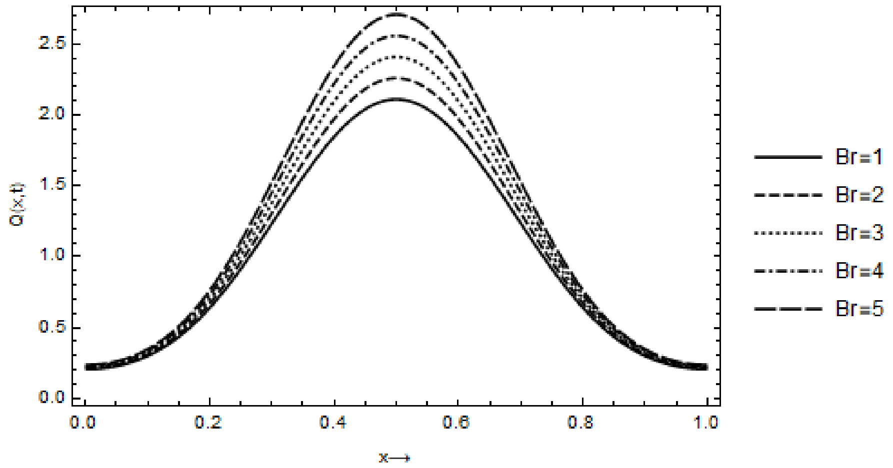

Fig 27 Effect on Brinkman number on Blood Flow Rate with other values $Gc=15, Gr=15, Pr=2.1, Sc=2, Rd_3=2, Rd_1=2, \omega=0.3, k=0.05, M=1.5$

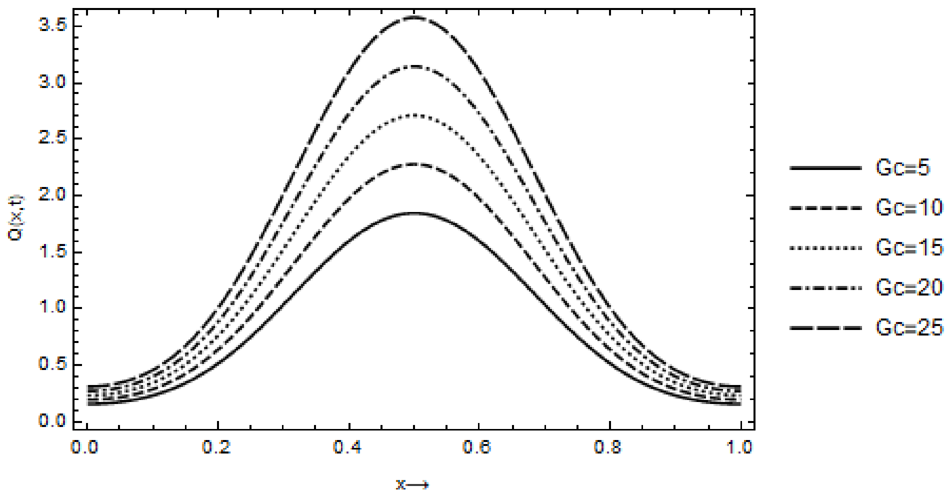

Fig 28 Effect of solutal Grashof number on Blood Flow Rate with other values $Br=5, Gr=15, Pr=2.1, Sc=2, Rd_3=2, Rd_1=2, \omega=0.3, k=0.05, M=1.5$

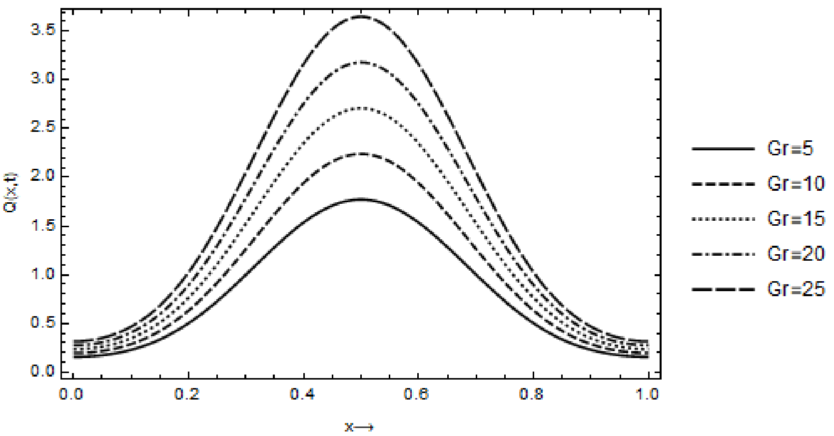

Fig 29 Effect of Grashof number on Blood Flow Rate with other values $Br=5, Gc=15, Pr=2.1, Sc=2, Rd_3=2, Rd_1=2, \omega=0.3, k=0.05, M=1.5$

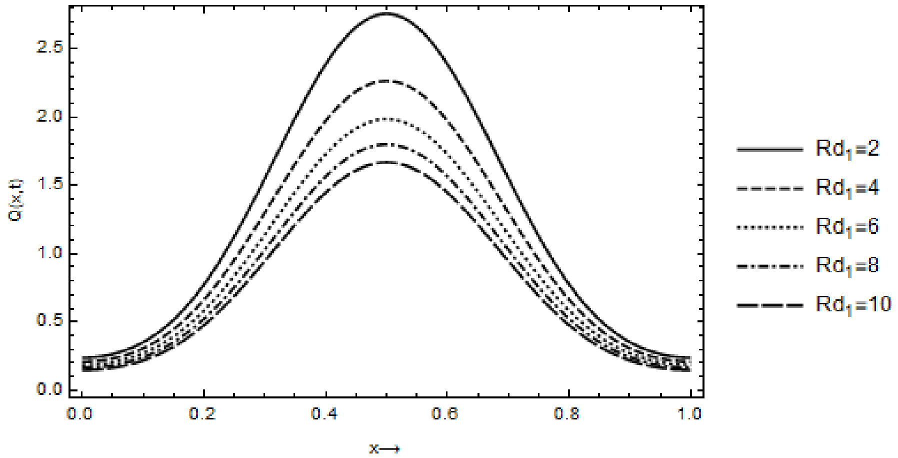

Fig 30 Effect of Radiation Absorption on Blood Flow Rate with other values
$Br = 5, Gc = 15, Gr = 15, Pr = 2.1, Sc = 2, Rd_3 = 2, \omega = 0.3, k = 0.05, M = 1.5$

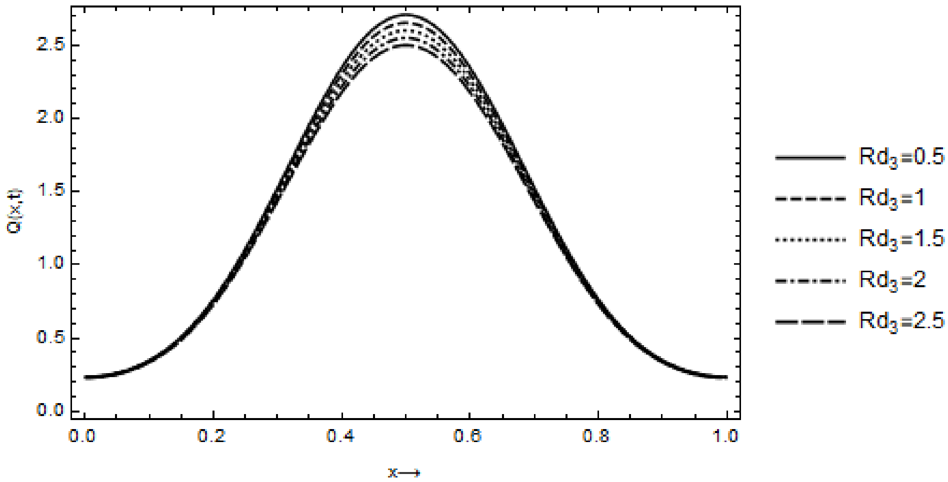

Fig 31 Effect of chemical reaction on Blood Flow Rate with other values
$Br = 5, Gc = 15, Gr = 15, Pr = 2.1, Sc = 2, Rd_1 = 2, \omega = 0.3, k = 0.05, M = 1.5$

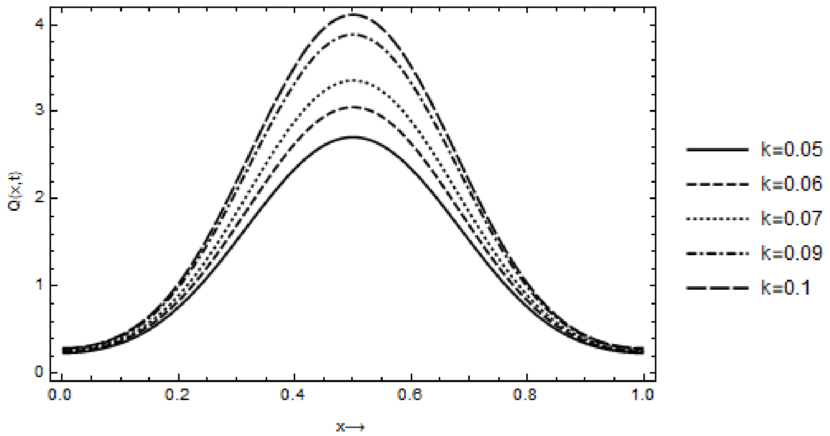

Fig 32 Effect of Porosity on Blood Flow Rate with other values
$Br = 5, Gc = 15, Gr = 15, Pr = 2.1, Sc = 2, Rd_3 = 2, Rd_1 = 2, \omega = 0.3, M = 1.5$

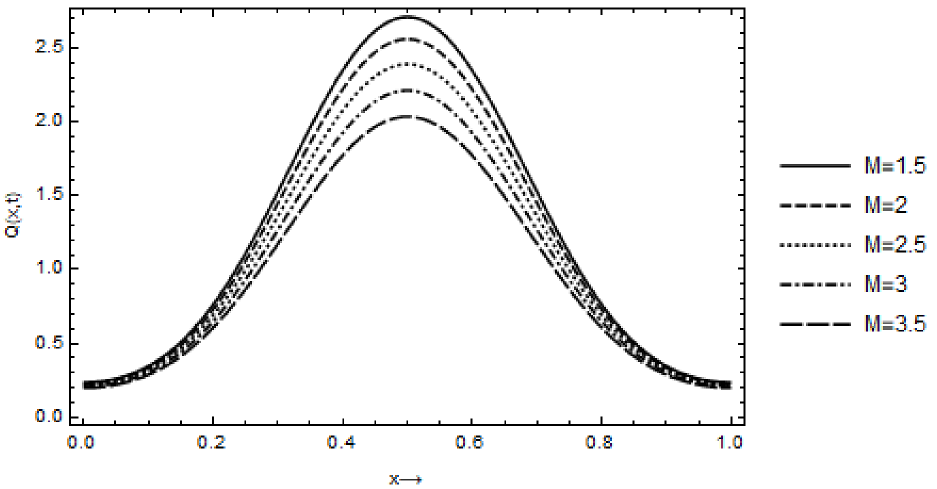

Fig 33 Effect of Magnetic Field on Blood Flow Rate with other values $Br=5, Gc=15, Gr=15, Pr=2.1, Sc=2, Rd_3=2, Rd_1=2, \omega=0.3, k=0.05$

6 Discussion

Fig 1 shows the effect of Schmidt number on lipid concentration in a sclerotic microchannel at a specific location $x=0.3$at the time $t=5$. The figure indicated that the lipid concentration decreases with an increase in Schmidt number, this increase in Schmidt number due to low kinematic viscosity and poor diffusivity.

Chemical reaction as result of other contributing parameter values is seen in Fig 2; the figure depicts that the lipid concentration decreases with an increase in chemical reaction at s specific location in the sclerotic artery.

Fig 3 illustrates the effect of the oscillatory frequency on lipid concentration in the blood. This result shows that the lipid concentration decreases with an increasing value of the oscillatory frequency at a specific location $x=0.3$. The concentration is maximum at the centre for different oscillatory frequency and converged at $r=0.893$.

The rate of mass transfer was investigated as depicted in Fig 4; the figure shows that mass transfer rate increases with different values of Schmidt number at different peak along the arterial channel while the other parameter values are $Rd_3=0.5, \omega=0.3$

The effect of chemical reaction on the rate of mass transfer was investigated as seen in Fig 5, the result shows that the rate of mass transfer increases with an increase in chemical reaction, with other parameter values are $Sc=0.2, \omega=0.3$along the arterial channel.

Fig 6 illustrates an effect of oscillatory frequency parameter change on rate of mass transfer along the sclerotic microchannel. This result is of the view that the mass transfer increases with an increasing value of the oscillatory frequency, with other values $Sc=0.2, Rd_3=0.5$along the sclerotic arterial channel.

Fig 7 shows the effect of Brinkman number on blood temperature in a sclerotic artery at a location $x=0.3$; the figure shows that the fluid temperature increases with an increase in Brinkman number.

The Schmidt number effect on blood temperature was depicted in Fig 8, and this result indicates that the blood temperature decreases with an increase in Schmidt number in the sclerotic artery at a specific location $x=0.3$. This result is an indication that the kinematic viscosity helps in reducing the temperature rise

Figs (9)-(12) show the effect of the Prandtl number, radiation absorption, chemical reaction parameter and oscillatory frequency parameter on the blood temperature. These results indicate that the blood temperature decreases with an increase in Prandtl number, radiation absorption, chemical reaction and oscillatory frequency at a specific location $x=0.3$in a sclerotic artery with treatment $R_T=4$ in time $t=5$.

Figs (13)-(18) illustrate the effects of Brinkman number, Schmidt number, Prandtl number, radiation absorption, chemical reaction and oscillatory frequency on the rate of heat transfer along sclerotic arterial channel. The results indicate that the rate of heat transfer increase with different values of the aforementioned parameters along the vessel at the treatment $R_T = 0.4$, growth rate $a = 0.34$.

The Brinkman number effect on blood flow was investigated as depicted by Fig 19; the figure shows that the velocity increases for an increase in Brinkman number with other parameter values $Gr = 15, Pr = 2.1, Sc = 2, Rd_3 = 2, Rd_1 = 2, \omega = 0.3, k = 0.05, M = 1.5$ at a specific location in the sclerotic microchannel.

Thermal Grashof number effect on blood velocity was investigated and result shown in Fig 20; the result shows that blood velocity increases with an increase in Grashof number at a specific location $x = 0.3$, with other parameter values such as $Gc = 15, Pr = 2.1, Sc = 2,\ Rd_3 = 2,\ Rd_1 = 2, \omega = 0.3, k = 0.05, M = 1.5,$ contributing to this flow behavior.

Fig 21 depicts the effect of Schmidt number on blood velocity in a sclerotic microchannel at a specific location $x = 0.3$. The figure shows that the blood velocity decreases with an increase in Schmidt number and the velocity decrease is due to low diffusivity.

The effect on Prandtl number on blood velocity was investigated as seen in Fig 22; the result shows that the velocity decreases for an increasing value of the Prandtl number.

Fig 23 illustrates the effect of radiation absorption on blood velocity in a sclerotic microchannel artery. It is seen that the blood velocity reduces as radiation absorption increases from $Rd_1 = 2, 4, 6, 8, 10$ at $x = 0.3$.

The chemical reaction as a result of the treatment and other contributing factors denoted with the parameters $Gc = 15, Gr = 15, Pr = 2.1, Sc = 2, Rd_1 = 2, \omega = 0.3, k = 0.05, M = 1.5,$ tends to reduce the velocity of the fluid in a sclerotic vessel as seen in Fig 24. The figure shows that blood velocity decreases for an increasing value of chemical reaction.

The study investigated the blood velocity at different of porosity in a sclerotic vessel as depicted by Fig 25. The figure shows that the blood velocity increases at different level of porosity, and it's maximum at the centre line of the artery for different porosity as well.

Fig 26 illustrates the effect of magnetic field on blood velocity at a specific location of $x = 0.3$ in the sclerotic microchannel at $t = 5$. In this figure, the axial velocity reduces with an increasing magnetic field parameter. This occurs due to the interaction of magnetic field with blood which produces body force called the Lorentz force, which impede the motion of blood in the vessel. The maximum velocity was observed at the centre line of the artery as depicted in the figure.

The research focuses on the effect of Brinkman number on blood flow; however, we investigated the effect of the Brinkman number on volumetric flow rate as seen in Fig 27. This figure indicates that the volumetric flow rate increases for an increase in Brinkman number. This useful flow rate behavior is made possible with the contribution of other pertinent parameters such as $Gc = 15, Gr = 15, Pr = 2.1, Sc = 2, Rd_3 = 2,$ $Rd_1 = 2, \omega = 0.3,\ k = 0.05,\ M = 1.5$.

Fig 28 indicates that the flow rate increases for different values of the solutal Grashof. The result is of the view that for us to increase the volumetric flow of viscous fluid as blood, we need to increase the solutal Grashof number which is due to the lipid concentration i the fluid. However, the flow is not complete without the contribution of other parameter values such as

$Br = 5, Gr = 15, Pr = 2.1, Sc = 2, Rd_3 = 2, Rd_1 = 2, \omega = 0.3, k = 0.05, M = 1.5$.

The thermal Grashof number was investigated along the arterial channel with other parameters values such as $Br = 5, Gc = 15, Pr = 2.1, Sc = 2, Rd_3 = 2,\ Rd_1 = 2, \omega = 0.3,\ k = 0.05,$

$M = 1.5$. This result is of the view that, the flow rate increases for different values of the thermal Grashof number as shown in Fig 29.

The radiation absorption was investigated and the result displayed in Fig 30, which shows that the flow rate decreases for an increase in radiation absorption with other parameters values $Br = 5, Gc = 15, Gr = 15, Pr = 2.1, Sc = 2, Rd_3 = 2, \omega = 0.3, k = 0.05, M = 1.5$ contributing to that flow behavior.

Fig 31 illustrates the blood volumetric flow rate for different values of the chemical reaction. This figure is of the views that increase in chemical reaction triggers a decrease in volumetric flow rate.

Fig 32 shows the blood flow rate for different values of the porosity in the blood vessel at $t = 5$ and the other contributing values are $Br = 5, Gc = 15, Gr = 15, Pr = 2.1, Sc = 2, Rd_3 = 2, Rd_1 = 2, \omega = 0.3, M = 1.5$. Magnetic field effect on flow rate was investigated as seen in Fig 33; the figure shows that the volumetric flow rate of blood decreases with increasing values of magnetic field along the arterial channel with treatment and growth rate of $R_T = 0.4$ and $a = 0.34$ respectively.

7 Conclusion

The radiation-brinkman number effects on blood flow in a porous atherosclerotic microchannel with the presence of a magnetic field, growth rate, and treatment. Using the Laplace method, the nonlinear partial differential equations with the effective governing parameters were examined. Our results were revealed as follows:

a. The axial velocity and volumetric flow decrease with the increase in Schmidt number, Prandtl number, radiation absorption, chemical reaction, magnetic field parameter. However, as the Brinkman number, solutal Grashof number, thermal Grashof number, and porosity parameter increase, so do the flow characteristics.

b. The cholesterol concentration decreases with an increase in Schmidt number, chemical reaction and oscillatory frequency, while the mass transfer rate increases with an increase in Schmidt number, chemical reaction and oscillatory frequency.

c. The blood temperature rises with an increase in Brinkman number but decreases with an increase in Schmidt number, Prandtl number, radiation absorption, chemical reaction, and oscillatory frequency, while the rate of heat transfers increases with an increase in Brinkman number, Schmidt number, Prandtl number, radiation absorption, chemical reaction, and oscillatory frequency.

Nomenclature

x^*	Dimensional coordinate along the channel
r^*	Dimensional coordinate perpendicular to the channel
R	Radius of an abnormal channel
R_0	Radius of normal channel
P_0	Systolic pressure
Rd_1	Radiation absorption parameter
Rd_3	Chemical reaction parameter
k_{Tb}	Blood thermal conductivity
w^*	Dimensional velocity profile
w	Dimensionless velocity profile

w_0 Perturbed velocity profile

C^* Dimensional lipid particle concentration

C_∞ Far field cholesterol particle concentration

c_{bp} The specific heat capacity of blood

t^* Dimensionless time

T Temperature of the fluid

T_∞^* Far field temperature

T_w^* Temperature at the wall

B_0 Magnetic intensity

M Magnetic field parameter

a Growth rate of LDL-cholesterol

Greek Symbols

υ_b Kinematic viscosity of blood

μ_b Dynamic viscosity of blood

Pr Prandtl number for blood

g Acceleration due to gravity

δ^* Dimensional height of stenosis

σ_e Electrical conductivity

λ^* Length of stenosis

ω Oscillatory frequency

θ Dimensionless blood temperature

ϕ Dimensionless cholesterol particle concentration

θ_a Dimensionless wall temperature

θ_0 Perturbed blood temperature profile

ϕ_a Dimensionless wall lipid concentration

ϕ_0 Perturbed lipid concentration

ρ_b Blood density

Subscripts

w Wall

b Blood

e Electrical

T Thermal

∞ Far field

MMDARG Mathematical Modeling and Data Analytic Research Group

References

1. Bunonyo, K. W., & Amos, E. (2020). Impact of Treatment Parameter on Blood Flow in an Atherosclerotic Artery. *American Journal of Theoretical and Applied Statistics*, *9*(3), 74.
2. Bunonyo, K. W., & Ebiwareme, L. (2022). Oscillatory Blood Flow and Embolitic Plaque Effect through a Microchannel with Metabolic Heat and Magnetic Field. *European Journal of Applied Physics*, *4*(1), 35-51.
3. Bhatti, M. M., Zeeshan, A., & Ellahi, R. (2016). Heat transfer analysis on peristaltically induced motion of particle-fluid suspension with variable viscosity: clot blood model. *Computer Methods and Programs in Biomedicine*, *137*, 115-124.
4. Lagendijk, J. J. W. (1982). The influence of bloodflow in large vessels on the temperature distribution in hyperthermia. *Physics in Medicine & Biology*, *27*(1), 17.
5. Srivastava, N. (2014). Analysis of flow characteristics of the blood flowing through an inclined tapered porous artery with mild stenosis under the influence of an inclined magnetic field. *Journal of Biophysics*, *2014*;1-9.
6. Bunonyo KW and Amos E. (2020). Investigation of treatment and radiation effects on oscillatory blood flow through a stenosed artery. American Journal of Engineering Research. 9(4);253-259.
7. Eldesoky, I. M. (2012). Slip effects on the unsteady MHD pulsatile blood flow through porous medium in an artery under the effect of body acceleration. *International Journal of Mathematics and Mathematical Sciences*, *2012*.
8. Makinde, O. D., & Mhone, P. Y. (2005). Heat transfer to MHD oscillatory flow in a channel filled with porous medium. *Romanian Journal of physics*, *50*(9/10), 931-938.
9. Hamza, M. M., Isah, B. Y., & Usman, H. (2011). Unsteady heat transfer to MHD oscillatory flow through a porous medium under slip condition. *International Journal of Computer Applications*, *33*(4), 12-17.
10. Choudhury, R., & Das, U. J. (2012). Heat transfer to MHD oscillatory viscoelastic flow in a channel filled with porous medium. *Physics Research International*, *2012*:1-5.
11. Biswas, D., & Chakraborty, U. S. (2009). Pulsatile flow of blood in a constricted artery with body acceleration. *Applications and Applied Mathematics: An International Journal (AAM)*, *4*(2), 8.
12. Hanvey RR, Khare RK and Paul A. (2017). Heat and mass transfer in oscillatory flow of a non-Newtonian fluid between two inclined porous plates placed in a magnetic field. *International Journal of Scientific and Engineering Research*. 8(7):1594-1597.
13. Plourde, B. D., Vallez, L. J., Sun, B., Nelson-Cheeseman, B. B., Abraham, J. P., & Staniloae, C. S. (2016). Alterations of blood flow through arteries following atherectomy and the impact on pressure variation and velocity. *Cardiovascular Engineering and Technology*, *7*(3), 280-289.
14. Ali, R., Kaur, R., Katiyar, V. K., & Singh, M. P. (2009). Mathematical modeling of blood flow through vertebral artery with stenoses. *Indian Journal of Biomechanics*, *151*, 151-158.
15. Mathur, P., & Jain, S. (2013). Mathematical modeling of non-Newtonian blood flow through artery in the presence of stenosis. *Advances in Applied Mathematical Biosciences*, *4*(1), 1.-1.
16. Aamir, A., & Saleem, A. (2011). Oscillatory channel flow for non-Newtonian fluid. *International Journal of Physical Sciences*, *6*(36), 8036-8043.

17. Varshney, G., Katiyar, V., & Kumar, S. (2010). Effect of magnetic field on the blood flow in artery having multiple stenosis: a numerical study. *International Journal of Engineering, Science and Technology*, *2*(2), 967-82.

18. Elangovan, K., & Selvaraj, K. (2017). MHD peristaltic flow of blood through porous medium with slip effect in the presence of body acceleration. *World Journal of Modelling and Simulation*, *13*(2), 151-160.

19. Sankad, G. C., & Nagathan, P. S. (2017). Transport of MHD couple stress fluid through peristalsis in a porous medium under the influence of heat transfer and slip effects. *International journal of applied mechanics and engineering*, *22*(2), 403-414.

20. Tripathi, B., & Sharma, B. K. (2018). Effect of variable viscosity on MHD inclined arterial blood flow with chemical reaction. *International Journal of Applied Mechanics and Engineering*, *23*(3).

21. Pralhad, R. N., & Schultz, D. H. (2004). Modeling of arterial stenosis and its applications to blood diseases. *Mathematical biosciences*, *190*(2), 203-220.

22. Bunonyo, K.W., and Amadi, U.C. (2022). Oscillatory electro-hydrodynamic (EHD) fluid flow through a microchannel in the presence of radiative heat and a magnetic field. *International Journal of Statistics and Applied Mathematics*. 7(3): 155-166

23. Bunonyo, K. W., & Eli, G. D. (2022). Convective Fluid Flow through a Sclerotic Oscillatory Artery in the Presence of Radiative Heat and a Magnetic Field. *Asian Journal of Pure and Applied Mathematics*, 258-278.